

Field-induced long-range magnetic order in the spin-singlet ground-state system YbAl_3C_3 : Neutron diffraction study

D. D. Khalyavin,^{1,*} D. T. Adroja,^{1,†} P. Manuel,¹ A. Daoud-Aladine,¹ M. Kosaka,² K. Kondo,² K. A. McEwen,³ J. H. Pixley,⁴ and Qimiao Si⁴

¹ISIS Facility, STFC, Rutherford Appleton Laboratory, Chilton, Didcot, Oxfordshire OX11 0QX, United Kingdom

²Department of Physics, Saitama University, Saitama 338-8570, Japan

³London Centre for Nanotechnology, and Department of Physics and Astronomy, University College London, Gower Street, London WC1E 6BT, United Kingdom

⁴Department of Physics and Astronomy, Rice University, Houston, Texas 77005, USA

(Received 9 February 2013; published 24 June 2013)

The $4f$ -electron system YbAl_3C_3 with a nonmagnetic spin-dimer ground state has been studied by neutron diffraction in an applied magnetic field. A long-range magnetic order involving both ferromagnetic and antiferromagnetic components has been revealed above the critical field $H_C \sim 6$ T at temperature $T = 0.05$ K. The magnetic structure indicates that the geometrical frustration of the prototype hexagonal lattice is not fully relieved in the low-temperature orthorhombic phase. The suppression of magnetic ordering by the remanent frustration is the key factor stabilizing the nonmagnetic singlet ground state in zero field. Temperature-dependent measurements in the applied field $H = 12$ T revealed that the long-range ordering persists up to temperatures significantly higher than the spin gap, indicating that this phase is not directly related to the singlet-triplet excitation. Combining our neutron diffraction results with the previously published phase diagram, we support the existence of an intermediate disordered phase as the first excitation from the nonmagnetic singlet ground state. Based on our results, we propose YbAl_3C_3 as a material for studying the quantum phase transitions of heavy-fermion metals under the influence of geometrical frustration.

DOI: [10.1103/PhysRevB.87.220406](https://doi.org/10.1103/PhysRevB.87.220406)

PACS number(s): 75.20.Hr, 75.25.-j, 75.30.Mb

The formation of a nonmagnetic singlet ground state due to spin dimerization is an extremely rare phenomenon in $4f$ -electron systems. It requires strong quantum effects which are usually significant only in low-dimensional spin $S = 1/2$ systems. Due to a larger total angular momentum J , and the three-dimensional character of interactions via conduction electrons, the spin dimer state is not favorable in most rare-earth compounds. The exceptional cases are Yb_4As_3 , where an effective spin $S = 1/2$ Heisenberg chain is believed to be realized¹ and the recently proposed spin-dimer system YbAl_3C_3 .²⁻⁵ Due to the effect of the crystalline electric field, the ground-state Kramers doublet is suggested to be well isolated from the excited states in these compounds and the $4f$ electrons at low temperature are expected to behave as a $S = 1/2$ spin system.

The nonmagnetic nature of the ground state in YbAl_3C_3 was initially interpreted as an antiferroquadrupolar ordered state⁶ which takes place at $T_S \sim 80$ K, where the specific heat exhibits a λ -type anomaly. Later, this interpretation was discarded by Ochiai *et al.*,² who observed a similar sharp peak in the specific heat for the Lu-based analog at 110 K and attributed it to a structural phase transition present in both compounds. The interpretation proposed by Ochiai *et al.*² implies formation of isolated dimers due to the structural distortions which promote the nonmagnetic spin-singlet ground state. This idea explains the low-temperature specific heat and magnetization data assuming the spin gap to be ~ 15 K. More direct evidence of the singlet-triplet excitations in YbAl_3C_3 has been presented by Kato *et al.*³ and Adroja *et al.*⁴ based on inelastic neutron scattering.

By analogy with insulating d -electron dimer systems, one can expect field-induced long-range magnetic order in

YbAl_3C_3 at the critical magnetic field closing the spin gap due to the Zeeman effect. It has been shown that this kind of quantum phase transition can be modeled as a Bose-Einstein condensation in a system of weakly interacting bosons.^{7,8} At the same time, the metallic nature of YbAl_3C_3 introduces an interplay between Ruderman-Kittel-Kasuya-Yosida (RKKY) and Kondo interactions which, in turn, suggests that the magnetic field will induce behavior that is distinct from that in insulating dimer systems. The aim of the present Rapid Communication, therefore, was to directly seek and investigate the field-induced long-range magnetic order in YbAl_3C_3 through neutron diffraction. Our data indeed reveal a change of the ground state from nonmagnetic below the critical field $H_C = 6$ T to magnetically ordered above H_C . Surprisingly, the suggested magnetic structure does not imply a strong exchange coupling for the expected isolated dimers and indicates the presence of geometrical frustration in spite of the lack of the threefold symmetry in the low-temperature structural phase. Based on the obtained results, one can conclude that the remanent frustration is the crucial ingredient promoting the low-temperature singlet ground state and is responsible for the unusual excitations in the system; in turn, our results suggest that YbAl_3C_3 provides a different setting to study heavy-fermion quantum phase transitions under the influence of geometrical frustration.

The high resolution neutron diffraction experiments were performed on a 2 g polycrystalline sample YbAl_3C_3 prepared as described by Kosaka *et al.*⁶ The measurements were carried out on the HRPD and WISH diffractometers⁹ at the ISIS Facility of the Rutherford Appleton Laboratory (UK).

The high-temperature neutron diffraction patterns ($T > 80$ K) can be successfully refined in the hexagonal

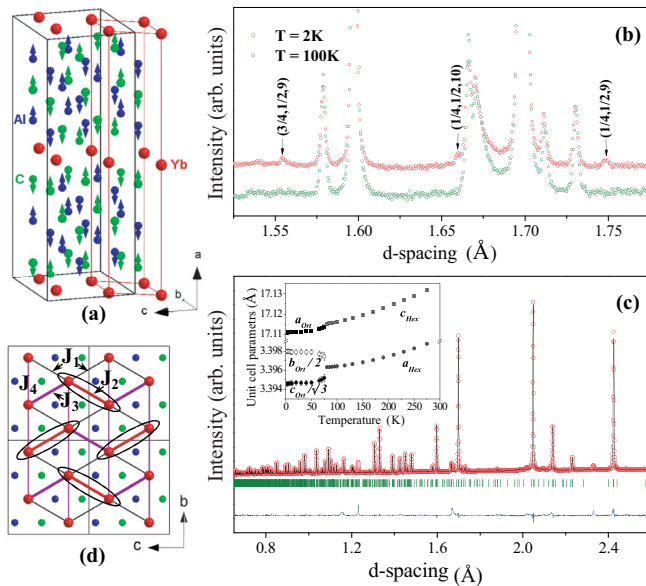


FIG. 1. (Color online) (a) Orthorhombic structure of YbAl_3C_3 (the parent hexagonal cell is shown as well). The primary orthorhombic displacements of Al and C are represented by arrows. (b) Neutron diffraction patterns collected above and below the structural phase transition. (c) Rietveld refinement of the neutron diffraction pattern collected at $T = 2$ K. The inset shows the unit cell parameters as a function of temperature. (d) Triangular layer formed by Yb^{3+} ions and the exchange parameters in the orthorhombic phase. J_2 bonds are arbitrarily taken to show the isolated dimers as ellipses around the bonds.

$P6_3/mmc$ space group, consistent with the previous diffraction studies.^{6,10} The structural parameters obtained at $T = 100$ K are summarized in the Supplemental Material.¹¹ The Yb^{3+} ions create two-dimensional triangular layers [Fig. 1(a)], causing the geometrical frustration for the associated $4f$ magnetic moments. The low dimensionality of the system is ensured by the large interlayer distance ~ 8.6 Å, resulting in a significant predominance of the in-plane interactions over the out-of-plane ones. Below T_S , a set of very weak additional reflections appears [Fig. 1(b)], indicating the structural phase transition. In agreement with the single crystal x-ray diffraction work by Matsumura *et al.*,¹² these reflections can be indexed with one of the symmetry related propagation vectors $\mathbf{k}_1 = 1/4, 1/4, 0$, $\mathbf{k}_2 = -1/4, 1/2, 0$, or $\mathbf{k}_3 = -1/2, 1/4, 0$. However, the atomic coordinates reported by these authors did not work with our diffraction data. To get a better structural model, a detailed symmetry analysis has been performed. The above-mentioned wave vector star combines four irreducible representations Λ_i ($i = 1-4$). For each representation, isotropy subgroups and displacive modes were generated using ISOTROPY (Ref. 13) and ISODISTORT (Ref. 14) software and checked in the refinement procedure, using the FullProf program,¹⁵ versus the experimentally measured superstructure reflections. We restricted our analysis by considering only subgroups associated with a single \mathbf{k} and $-\mathbf{k}$ pair, as experimentally found by Matsumura *et al.*¹² The analysis resulted in the conclusion that the displacive modes involving only Al and C and associated with the Λ_3 representation and the $(a, 0, 0, a, 0, 0)$

order parameter direction drive the phase transition at T_S . These primary modes have the $Pbca$ symmetry in agreement with the reflection conditions deduced by Matsumura *et al.*¹² and induce the atomic displacements along the hexagonal c axis [Fig. 1(a)]. We found the Yb ions were not displaced within the precision of our diffraction experiment. Taking into account this result, the final refinement [Fig. 1(c)] was done in the orthorhombic $Pbca$ space group (related to the hexagonal $P6_3/mmc$ by $\mathbf{a}_0 = \mathbf{c}_h$, $\mathbf{b}_0 = 2\mathbf{a}_h + 2\mathbf{b}_h$, and $\mathbf{c}_0 = \mathbf{b}_h - \mathbf{a}_h$) using only four parameters varying the x coordinates for the six nominally independent Al and C sites. The y and z coordinates for these atoms as well as all coordinates for Yb were fixed to their high symmetry values corresponding to the high-temperature hexagonal phase.¹¹ This simplified approach to the refinement of the low-temperature phase is the only one possible due to the limited number of superstructure reflections in the powder data allowing us to determine only primary distortions.

Considering the effect of the symmetry lowering on the exchange topology of the Yb sublattice, the favorable symmetry conditions to form isolated dimers should be pointed out. In the low-temperature orthorhombic phase there are four nonequivalent in-plane exchange couplings shown in Fig. 1(d). J_2 and J_3 form isolated dimers and can potentially promote the nonmagnetic singlet ground state. The corresponding Yb-Yb interatomic distances vary only slightly due to the small variations of the a and b unit cell parameters [Fig. 1(c) inset], which indicates that the main factor renormalizing the exchange parameters should be related to the Al and C displacements.

The absence of any sign of long-range magnetic ordering in our experiment down to 0.05 K is fully consistent with the previous neutron diffraction,⁶ Mössbauer spectroscopy,¹⁶ and muon spin relaxation¹⁷ studies. However, application of magnetic field ~ 6 T changes the nonmagnetic ground state of YbAl_3C_3 . A clear ferromagnetic signal on top of some nuclear peaks and a set of additional reflections in a low- Q region [Fig. 2(a)] indicate the onset of long-range magnetic order. The field dependence of both ferromagnetic [Fig. 2(c)] and antiferromagnetic [Fig. 2(b)] components demonstrates a critical behavior with the critical exponents 0.24(3) and 0.32(6), respectively. The quantitative refinement of the magnetic intensity [Fig. 2(d)] revealed a uniform ferromagnetic component along the orthorhombic c axis and an antiferromagnetic component along the b axis. The latter does not require enlargement of the orthorhombic nuclear unit cell and all magnetic peaks can be indexed with the $\mathbf{k} = 0$ propagation vector. Using representation theory,^{13,14} we classified different magnetic configurations according to irreducible representations of the $Pbca$ space group and used them in the refinement procedure. A solution within a single irreducible representation could not be found, therefore combinations of different representations were tested. We found that many combinations describe the observed magnetic intensities equally well [Fig. 2(d)] and no unique solution can be deduced from the powder data. However, the important point is that all these solutions can be presented as admixtures of two configurations denoted as A and B in Fig. 3 (top) and representing magnetic ordering in the triangular layers. It can be a simple interchanging of these layers, $[A]_{x \sim 0} \rightarrow$

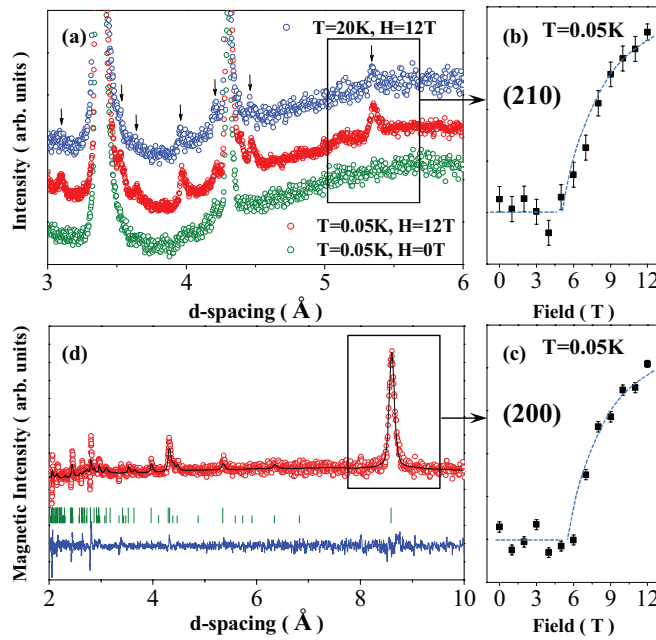


FIG. 2. (Color online) (a) Neutron diffraction patterns collected at different temperatures and magnetic fields. The arrows indicate the positions of the additional reflections induced by the magnetic field. (b) Integrated intensity of the antiferromagnetic peak (210) as a function of the magnetic field. (c) Ferromagnetic contribution to the (200) nuclear reflection as a function of the magnetic field. (d) Refinement of the magnetic intensities obtained by subtraction of the patterns collected at $T = 0.05$ K in $H = 12$ and 0 T (magnetic Bragg factor $R_{\text{Bragg}} = 6.2\%$).

$[B]_{x \sim 0.5} \rightarrow [A]_{x \sim 1} \rightarrow \dots$, along the orthorhombic a axis (the former hexagonal c axis), which in combination with the ferromagnetic component results in the canted structure (Fig. 4 inset) with monoclinic $P2'_1$ symmetry, or a more complex orthorhombic $P2'_12'_12_1$ combination involving disordered antiferromagnetic components on half of the Yb sites (Fig. 3 bottom) and implying $[A - B]_{x \sim 0} \rightarrow [A + B]_{x \sim 0.5} \rightarrow [A - B]_{x \sim 1} \rightarrow \dots$ alternation. Practically, it means interchanging two types of the triangular layers; one of them is randomly represented by the A or B configurations taken with different signs, and the second one is randomly represented by these configurations taken with the same sign. There are many intermediate situations with sites half fully ordered and half partially ordered (intermediate between the structures shown in Fig. 4). However, the most symmetric variant $P2'_12'_12_1$ is considered to be preferable since it involves only two representations and therefore a lower degree of degeneracy. The value of the ordered moments for Yb^{3+} ions depends on the model and varies from $2.3(3)\mu_B$ for the fully ordered configurations up to $2.7(3)\mu_B$ for the partially disordered ones with only half of the sites carrying the ordered antiferromagnetic component.

The admixture of the A and B configurations signifies their degeneracy and points to the fact that the geometrical frustration is not fully relieved by the structural phase transition at T_S . Quantitatively, the frustration can be expressed by the ratio $(J_2 + J_3)/2 = J_1$ between the in-plane exchange parameters, which is held in the orthorhombic phase. This

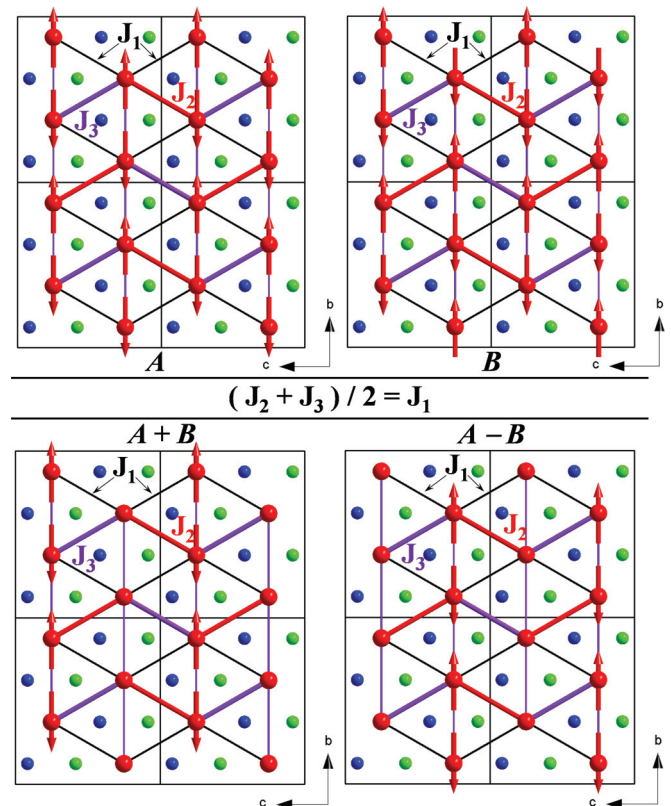


FIG. 3. (Color online) Top: Two degenerate spin configurations denoted as A and B in a triangular layer. Bottom: Superposition of these configurations taking with the same (left) and opposite signs (right).

ratio is not consistent with the strong predominance of either J_2 or J_3 exchange coupling expected from the symmetry arguments to form isolated dimers. A possible explanation of this experimental fact is that the ground state of Yb^{3+} ions in the field-induced ordered phase is essentially different from the zero-field singlet state. This assumption comes from the large ordered moment of Yb obtained from the experimentally measured magnetic intensities. The new ground state adopts the bigger moment to gain full advantage of the magnetically ordered state and can renormalize the exchange parameters in the system.

The results obtained indicate directly that the frustrated nature of the orthorhombic phase is the key factor to stabilize the nonmagnetic singlet ground state in YbAl_3C_3 , as it has been originally suggested by Kato *et al.*³ The magnetic fluctuations between degenerate manifolds caused by the frustration prevents the system from choosing a unique ordered pattern and the spin dimerization takes place to lift the degeneracy of the ground state.

Field-induced transitions to magnetically ordered phases are commonly observed in many d -electron dimer systems.⁸ However, in strong contrast with these systems, YbAl_3C_3 does not show a cusp in magnetization curves measured in fields $H > H_C$ as a function of temperature,⁵ which can be attributed to the onset of magnetic ordering at the critical temperature $T_N(H)$. To clarify this important issue, we performed temperature-dependent diffraction measurements

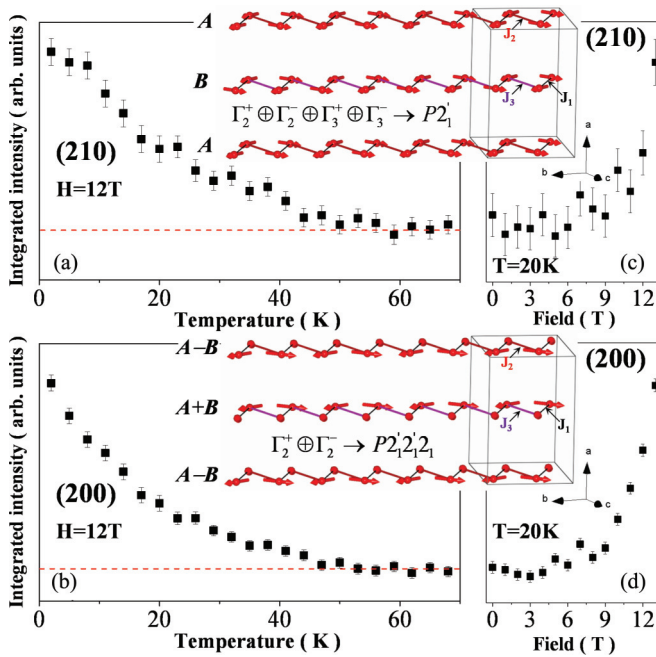


FIG. 4. (Color online) Integrated intensities of the (a) (210) antiferromagnetic and (b) (200) ferromagnetic reflections measured in applied magnetic field $H = 12$ T as a function of temperature. (c) and (d) show these reflections as a function of magnetic field at $T = 20$ K. The inset shows two examples of the field-induced magnetic structures combining degenerate A and B triangular layers. The monoclinic $P2'_1$ structure (top) is fully ordered, and the ferromagnetic (along the c axis) and antiferromagnetic (along the b axis) components equal $1.6(2)\mu_B$ and $1.6(2)\mu_B$, respectively, in the magnetic field $H = 12$ T. The orthorhombic $P2'_12'_12_1$ structure (bottom) consists of a fully ordered ferromagnetic component, $1.6(2)\mu_B$, and a partially disordered antiferromagnetic one, $2.2(2)\mu_B$ (only half of the sites carry a nonzero antiferromagnetic component).

in the magnetic field $H = 12$ T applied at 0.05 K. Surprisingly, both the ferromagnetic and antiferromagnetic contributions to the Bragg peaks do not show a clear critical behavior [Figs. 4(a) and 4(b)]. They gradually decrease and vanish at about the same temperature ~ 50 K. The observation of the magnetic scattering at such high temperatures indicates that the field-induced long-range magnetic order is not directly related to the singlet-triplet excitation since it can be induced at temperatures significantly higher than the spin gap. The critical field increases with temperature and is ~ 9 T at $T = 20$ K [Figs. 2(a), 4(c), and 4(d)]. The observed temperature dependence of the magnetic intensities is therefore dominated by the increase of the critical field with temperature. Precise determination of the phase diagram from powder measurements requires an unreasonably larger amount of beamtime and can only be done in a single crystal experiment. Above 50 K, the critical field becomes bigger than 12 T and is beyond the capabilities of our experimental setup. Apparently the field-induced phenomenon is closely related to the structural phase transition at $T_S \sim 80$ K and the long-range ordered phase can be induced below this critical temperature.

Taking into account the frustrated nature of the YbAl_3C_3 crystal structure and the strong antiferromagnetic interactions

(the paramagnetic Curie temperature is ~ -100 K), the system is expected to be in a “classical” spin-liquid regime in a wide temperature range below T_S . Thus, the field-induced long-range magnetic order can be associated with the properties of this phase rather than with the singlet-triplet excitation. This consideration presumes that the spin dimerization takes place from the disordered spin-liquid phase, in other words, the nonmagnetic quantum singlet state competes with this phase and therefore one can expect that the first excitation, when the spin gap is closed, is the disordered spin-liquid phase as well. The long-range ordering therefore is the second excited state. The presence of the intermediate field-induced disordered phase at low temperatures cannot be directly deduced from the powder diffraction data since this phase does not contribute to the Bragg diffraction, but the recent single crystal magnetization data reported by Hara *et al.*⁵ clearly indicates the presence of the intermediate phase below 6 T. This intermediate phase indeed has been recently confirmed through an inelastic neutron scattering study in an applied magnetic field by Adroja *et al.*,⁴ which revealed that the position and intensity of the inelastic excitations changed dramatically between $H = 3$ and 5 T.

The metallic nature of YbAl_3C_3 suggests the importance of the Kondo effect and its interplay with RKKY interactions. We therefore expect it to be a material that can be used to study the global phase diagram of antiferromagnetic heavy-fermion metals.^{18,19} There is a burst of recent interest in studying such a phase diagram through materials that can tune the degree of local-moment quantum fluctuations through dimensionality²⁰ or geometrical frustration.^{21–23} YbAl_3C_3 belongs to the latter class of materials, with the distinction that the relevance of geometrical frustration is explicitly established even though the system is metallic. Further support for our picture comes from the observation of a large value of the Sommerfeld coefficient ($\gamma = C/T$)⁵ at intermediate magnetic fields.

In conclusion, our neutron diffraction study revealed that application of a magnetic field above $H_C \sim 6$ T induces long-range magnetic order in YbAl_3C_3 at $T = 0.05$ K. The magnetic structure involves a homogeneous ferromagnetic component along the orthorhombic c axis and an antiferromagnetic component along the b axis. The latter is likely to be disordered on half of the Yb sites. In the magnetic field $H = 12$ T, both the ferromagnetic and antiferromagnetic components persist up to 50 K, indicating that the long-range order is not directly related to the singlet-triplet excitation. A field-induced intermediate disordered phase is likely to exist as the first excitation from the nonmagnetic singlet ground state. This opens the primary question whether the long-range magnetically ordered phase in YbAl_3C_3 really displays similar physics to that of a Bose-Einstein condensation of magnons and how the Kondo effect interplays with the magnetic frustration.

We would like to thank A. D. Hillier, J.-G. Park, J. R. Stewart, T. Guidi, and P. Riseborough for interesting discussions. D.T.A. would like to acknowledge financial assistance from CMPC-STFC Grant No. CMPC-09108. The work at Rice has been supported in part by NSF Grant No. DMR-1006985 and Robert A. Welch Foundation Grant No. C-1411.

*dmitry.khalyavin@stfc.ac.uk

†devashibhai.adroja@stfc.ac.uk

- ¹M. Kohgi, K. Iwasa, J.-M. Mignot, A. Ochiai, and T. Suzuki, *Phys. Rev. B* **56**, R11388 (1997).
- ²A. Ochiai, T. Inukai, T. Matsumura, A. Oyamada, and K. Katoh, *J. Phys. Soc. Jpn.* **76**, 123703 (2007).
- ³Y. Kato, M. Kosaka, H. Nowatari, Y. Saiga, A. Yamada, T. Kobiyama, S. Katano, K. Ohyama, H. S. Suzuki, N. Aso, and K. Iwasa, *J. Phys. Soc. Jpn.* **77**, 053701 (2008).
- ⁴D. T. Adroja *et al.*, ISIS, Experimental Report No. RB920466, 2010 (unpublished); ISIS, Experimental Report No. RB1210320, 2013 (unpublished).
- ⁵K. Hara, S. Matsuda, E. Matsuoka, K. Tanigaki, A. Ochiai, S. Nakamura, T. Nojima, and K. Katoh, *Phys. Rev. B* **85**, 144416 (2012).
- ⁶M. Kosaka, Y. Kato, C. Araki, N. Mori, Y. Nakanishi, M. Yoshizawa, K. Ohoyama, C. Martin, and S. W. K. Tozer, *J. Phys. Soc. Jpn.* **74**, 2413 (2005).
- ⁷T. Nikuni, M. Oshikawa, A. Oosawa, and H. Tanaka, *Phys. Rev. Lett.* **84**, 5868 (2000).
- ⁸T. Giamarchi, C. Ruegg, and O. Tchernyshyov, *Nat. Phys.* **4**, 198 (2008).
- ⁹L. C. Chapon, P. Manuel, P. G. Radaelli *et al.*, *Neutron News* **22**, 22 (2011).
- ¹⁰T. M. Gesing, R. Potgen, W. Jeitschko, and U. Wortmann, *J. Alloys Compd.* **186**, 321 (1992).
- ¹¹See Supplemental Material at <http://link.aps.org/supplemental/10.1103/PhysRevB.87.220406> for structural parameters of YbAl₃C₃.
- ¹²T. Matsumura, T. Inami, M. Kosaka, Y. Kato, T. Inukai, A. Ochiai, H. Nakao, Y. Murakami, S. Katano, and H. S. Suzuki, *J. Phys. Soc. Jpn.* **77**, 103601 (2008).
- ¹³H. T. Stokes, D. M. Hatch, and B. J. Campbell, ISOTROPY, [stokes.byu.edu/isotropy.html].
- ¹⁴B. J. Campbell, H. T. Stokes, D. E. Tanner, and D. M. Hatch, *J. Appl. Crystallogr.* **39**, 607 (2006).
- ¹⁵J. Rodriguez Carvajal, *Physica B* **193**, 55 (1993).
- ¹⁶S. K. Dhar, P. Manfrinetti, M. L. Fornasini, and P. Bonville, *Eur. Phys. J. B* **63**, 187 (2008).
- ¹⁷T. Yoshida, T. Endo, H. Fujita, H. Nowatari, Y. Kato, M. Kosaka, K. Satoh, T. U. Ito, and W. Higemoto, Meet. Abstr. Phys. Soc. Jpn. **61**, 414 (2006).
- ¹⁸Q. Si, *Physica B* **378**, 23 (2006); *Phys. Status Solidi B* **247**, 476 (2010).
- ¹⁹P. Coleman and A. H. Nevidomskyy, *J. Low Temp. Phys.* **161**, 182 (2010).
- ²⁰J. Custers *et al.*, *Nat. Mater.* **11**, 189 (2012).
- ²¹M. S. Kim and M. C. Aronson, *Phys. Rev. Lett.* **110**, 017201 (2013).
- ²²V. Fritsch *et al.*, arXiv:1301.6062.
- ²³E. D. Mun, S. L. Budko, C. Martin, H. Kim, M. A. Tanatar, J.-H. Park, T. Murphy, G. M. Schmiedeshoff, N. Dilley, R. Prozorov, and P. C. Canfield, *Phys. Rev. B* **87**, 075120 (2013).